Kinetic simulation of magnetic field generation via the Biermann Battery effect for laser-driven HED experimental conditions

Jill Peery[1], Jack Matteucci[2], Will Fox[2], Derek Schaeffer[2], Kirill Lezhnin[2]
[1] Willamette University [2]Princeton Plasma Physics Laboratory

Biermann Battery Effect

This project hopes to characterize the magnetic field generated by the Biermann Battery Effect in high energy density (HED) plasma regimes, with respect to varying experimental conditions.

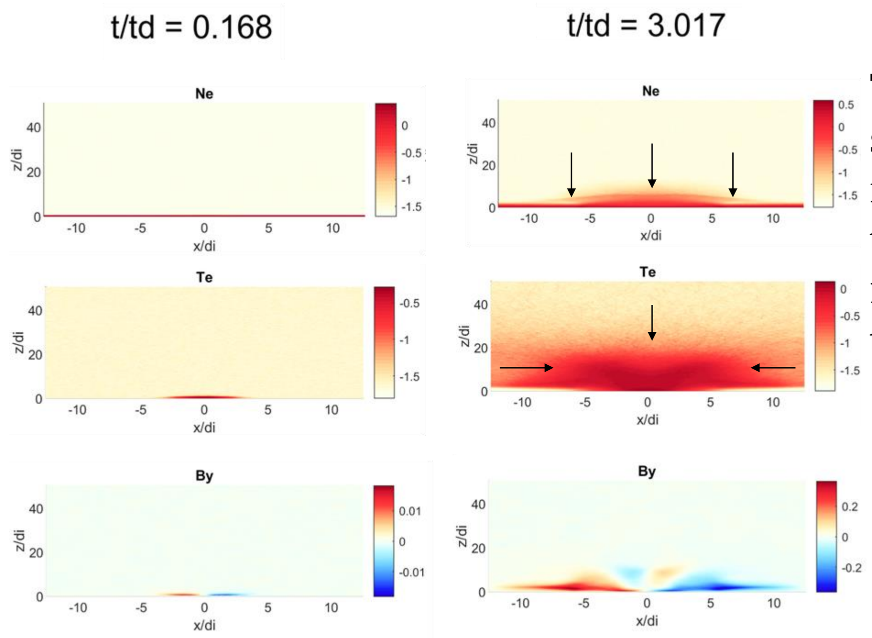

Figure one shows density, temperature and magnetic field at two points in time for the Nilson case. Arrows indicate density and temperature gradients

The Biermann Battery Effect is the spontaneous generation of a magnetic field in a plasma. It occurs when the temperature and density gradients are non-collinear. It's derived from a term in the curl of Ohm's law as follows:

$$\frac{\partial B}{\partial t} = \nabla \times \frac{1}{n_e e} \nabla P_e$$

$$\frac{\partial B}{\partial t} = \nabla \frac{1}{n_e e} \times \nabla T_e n_e$$

$$\frac{\partial B}{\partial t} = -\frac{1}{n_e e} \nabla n_e \times \nabla T_e$$

Biermann Term

To characterize the magnetic field, we used PSC, a fully kinetic particle-in-cell (PIC) code. With the code, we modeled the Nilson Case[1], an HED experiment where a plasma plume is ablated from a flat target by a high intensity laser and expands into a background plasma of lower density.

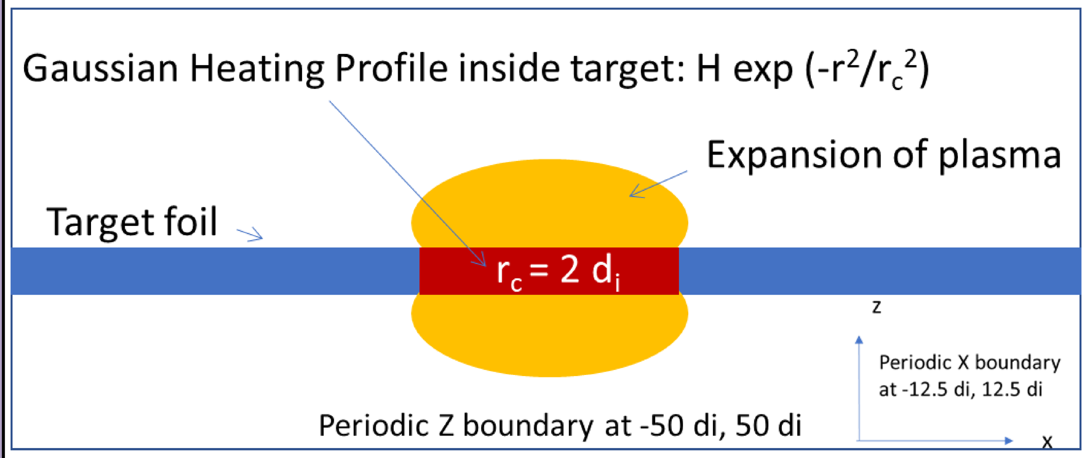

Figure two shows a 2d view of the full area for the starting setup of the Nilson Case.

We determined the effect of experimental conditions by varying the parameters' values from those used in the Nilson case. In each scan, all other parameters were kept at their original value. The parameters scanned in this project are listed below.

Parameter:	Original value:
• Collisionality	*Lambda0=20*
• Laser Heating Profile	*K=2*
• Laser Heating Radius	*rH=3*
• Ion Species	*Z=1*
• Background Density	*nb=0.01*

A characterization of the Biermann generation based on these parameters will be immediately relevant in HED experiments, applicable to research on inertial confinement fusion and also in astrophysical research, where the Biermann Battery effect is important in dynamo theories as a possible source for seed magnetic fields.

1. Nilson P M *et al* 2006 *Phys. Rev. Lett.* **97** 255001

Generalized Curl of Ohm's Law

The Biermann term is found in the Curl of Generalized Ohm's law

Term 1 Term 2 Term 3 Term 4 Term 5

$$\frac{\partial B}{\partial t} = \nabla \times (V_i \times B - \frac{J}{e n_e} \times B + \frac{1}{n_e e}\nabla P_e + \frac{1}{n_e e}\nabla \cdot \Pi - \frac{1}{n_e e} R_{ei}$$

- Term 1, curl of VxB: Advection due to Ion Flow
- Term 2, curl of JxB: Advection due to Hall Current
- Term 3: Biermann Battery Term
- Term 4: Traceless Pressure Contribution (Weibel, Reconnection)
- Term 5, curl of REI: Electron/Ion Momentum exchange (Magnetic Diffusion, Nernst advection)

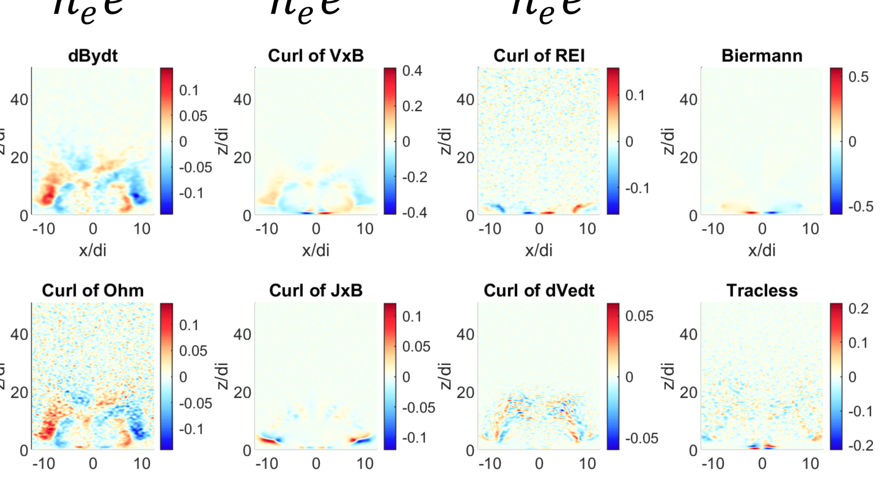

Figure three shows the individual curl of Ohm's Law terms calculated for the Nilson Case at t=5.196.

Results

In PSC, we track density, temperature and magnetic field (Fig.1), the change in magnetic field caused by each of the terms of Ohm's law as well as the total change in magnetic field (Fig.3) at each time step. We also track the values shown in Fig.4 that give additional necessary information about the magnetic fields.

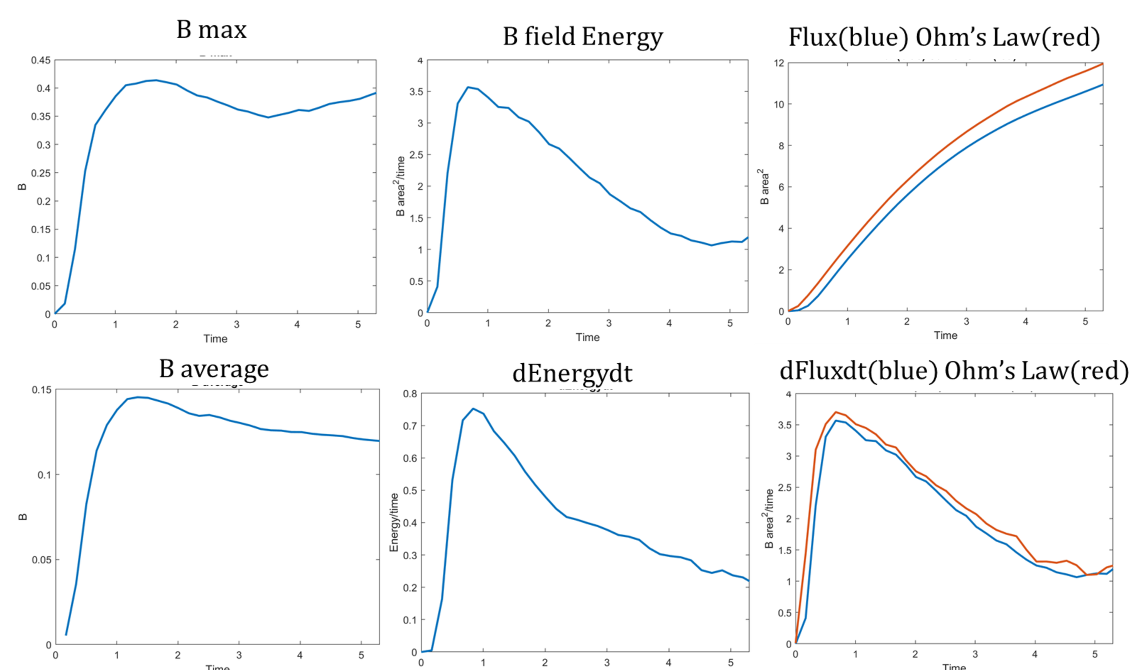

Figures four-nine shows plots of max and average magnetic field, magnetic energy and change in energy, and magnetic flux and change in flux vs time for the Nilson case. Flux and change in flux have 2 lines plotted to show the two different ways these values are calculated.

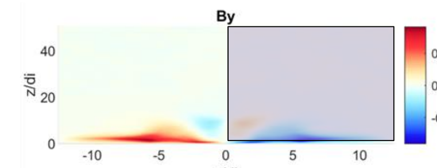

Figure 10 shows area integrated over

The space integrated values (Flux, dFluxdt, Energy and dEnergydt) were calculated across ¼ of the total area simulated, as shown by the shaded area in Fig. 10. The average field was found by taking the average over only cells where a non-trivial field was present.

The Effect of Collisionality on Magnetic Field Generation

Collisionality is controlled in PSC using the variable Lambda0 $= \frac{mean\ free\ path}{electron\ inertial\ length}$

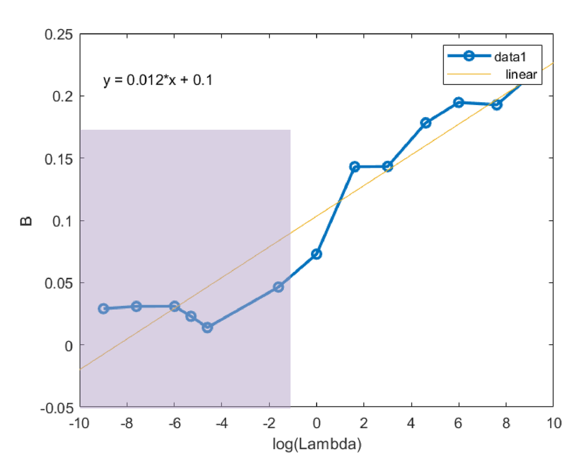

Figure 10 shows the max magnetic field and a fitted trend line that is linear with respect to log of Lambda0.

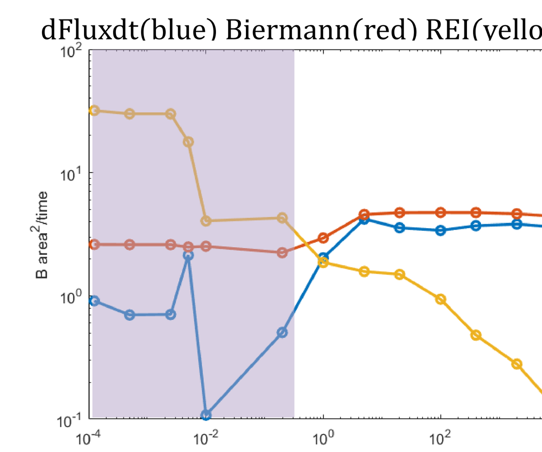

Figure 11 shows instantaneous magnetic flux, Biermann generation and REI contribution over a range of Lambda0 from 0.000125 to 8000.

We see a trend of decreasing magnetic field with increasing collisionality, as increasing collisionality is accompanied by magnetic diffusion and resistivity that dissipate the magnetic field. At high collisionalities (Lambda0<1) we found that the REI term was much higher than it should be and overwhelmed the other terms from the Curl of Ohm's law. The data at these collisionalities, indicated by the shading, is untrustworthy and still under study.

The Effect of Laser Heating Profile on Magnetic Field Generation

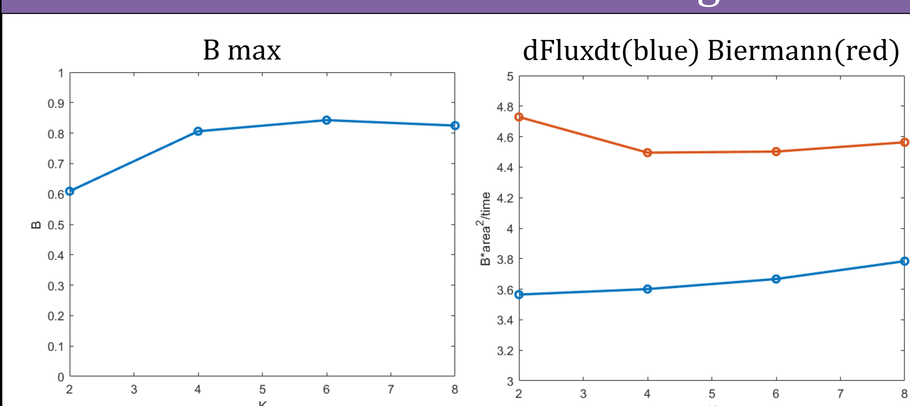

In PSC, the heating profile of the laser onto the target is a gaussian. We change the power in the exponent, denoted by the variable K, to alter the profile. We found that varying K had negligible effect on both Biermann generation and max magnetic field.

Figures 12 and 13 show that max magnetic field, and the instantaneous flux and Biermann generation are constant as K is varies between 2 and 8.

The Effect of Laser Heating Radius on Magnetic Field Generation

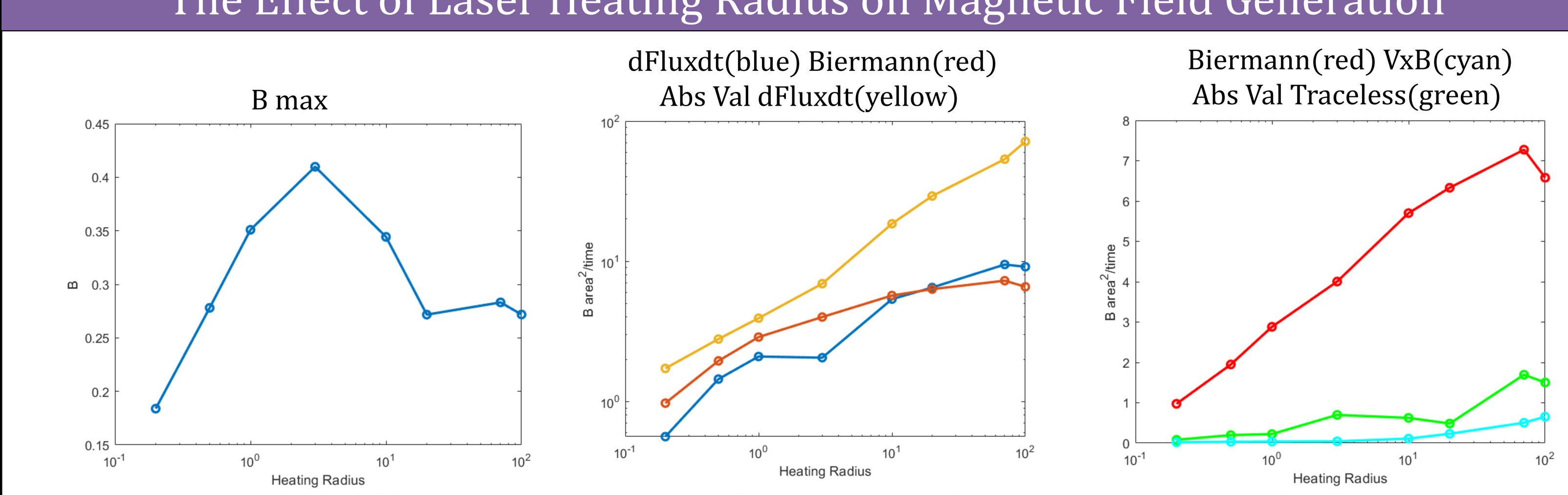

Figure 14 shows max magnetic field as heating radius varies from 0.2 to 100. Figure 15 shows instantaneous magnetic flux and Biermann generation, and the absolute value of instantaneous flux. Figure 16 shows instantaneous flux contributions from the Bierman, vxb and absolute value of traceless pressure terms

Results

As we increased the radius of the heated spot on the target, we found that the max magnetic field reached a peak and then decreased. We also found at these radii, that the absolute value of dFluxdt was much larger than dFluxdt. These results are caused at least in part the appearance of ion Weibel instability, which begins to dominate field generation at rH>>d_i.

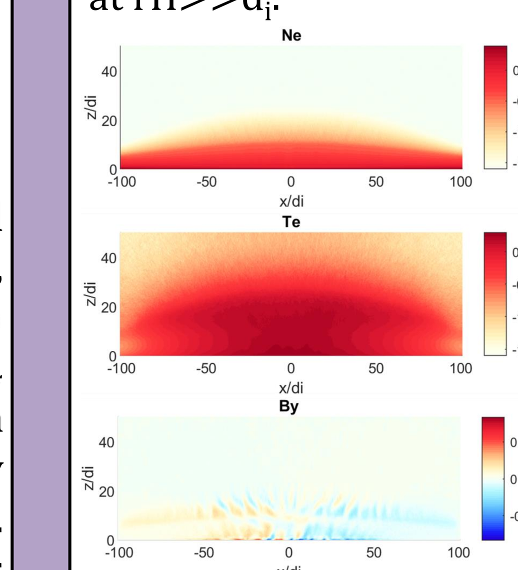

Figure 17 shows density, temperature and magnetic field for rH=100 at t=4.16.

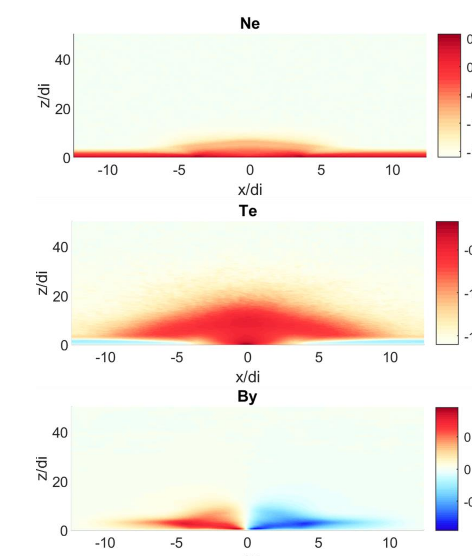

Figure 18 shows density, temperature and magnetic field for rH=0.5 at t=4.16.

Weibel instability can be seen in the magnetic field at rH=100. It does not appear in the field at rH closer to d_i. We are continuing to look into these results.

The Effect of Ion Species on Magnetic Field Generation

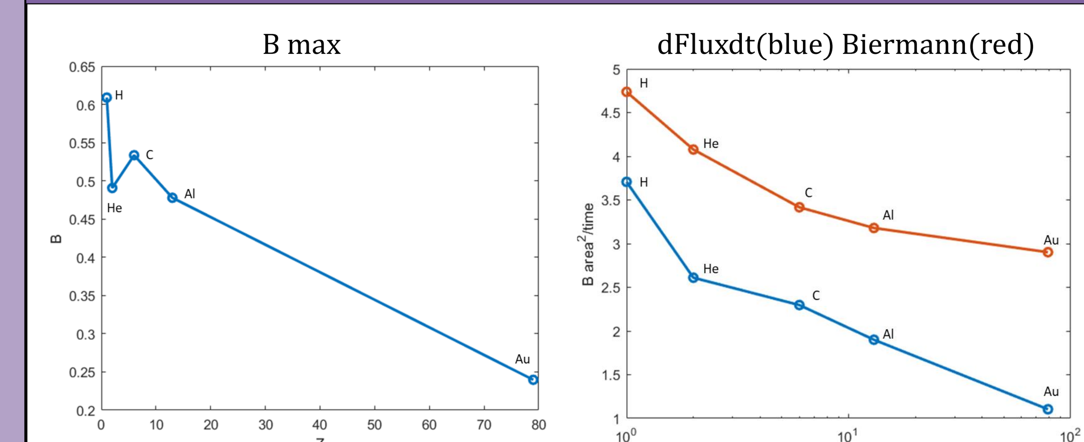

Figures 19 and 20 show max magnetic field, instantaneous magnetic flus and Biermann generation for ions from H to Au.

We changed atomic number Z in PSC to scan ion species for Hydrogen, Helium, Carbon, Aluminum and Gold. We found a general decreasing trend in max magnetic field and Biermann generation as Z was increased.

The Effect of Background Plasma Density on Magnetic Field Generation

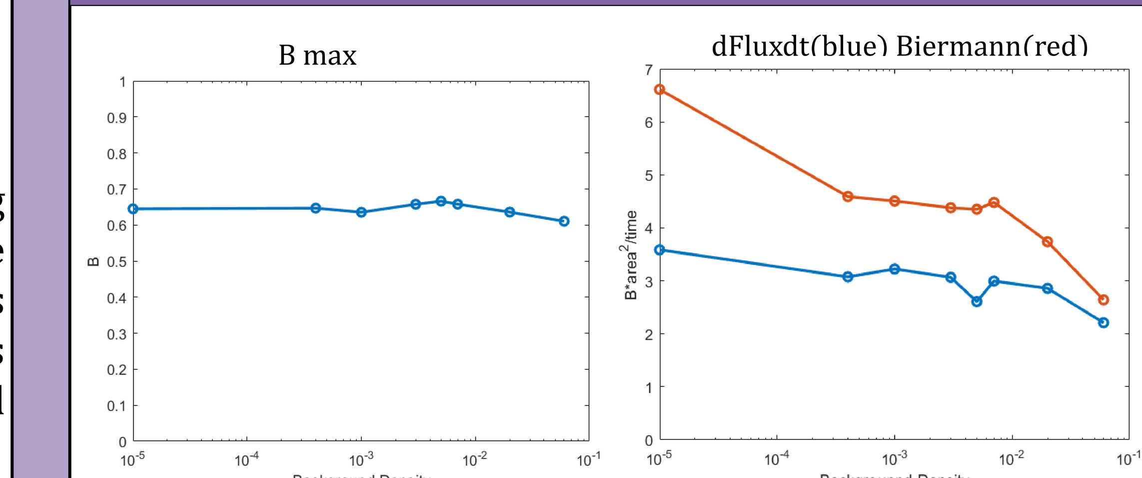

Figures 21 and 22 show the max magnetic field, and the instantaneous flux and Biermann generation for background density in a range from vacuum to 0.1.

The background density is represented by the variable nb and is in relation to the density of the target, which has nb=1. Max magnetic field was found to be not affected meaningfully by variation of background plasma density. Biermann magnetic field generation decreased with increasing background density as the density gradient between the target and the background became smaller.

Future Work

- Further examination of collisionality, laser heating radius and ion species scans (collection of more data points)
- Similar examinations of other experimental conditions
- Comparison of this data to results from MHD simulations
- Comparison of this data to results from previous experiments relating to the Biermann Battery Effect.

Acknowledgments

PPPL